ELSEVIER

Journal of Fluids and Structures 24 (2008) 436–445

JOURNAL OF FLUIDS AND STRUCTURES

www.elsevier.com/locate/jfs

Brief Communication

A nonlinear analysis of stability and gust response of aeroelastic systems

D. Dessi[a,*], F. Mastroddi[b]

[a]*Department of Vibration and Noise, Istituto Nazionale per Studi ed Esperienze di Architettura Navale (INSEAN), Via di Vallerano 39, 00128, Rome Italy*

[b]*Department of Aerospace Engineering and Astronautics, University of Rome "La Sapienza", Via Eudossiana 16, 00184 Rome Italy*

Received 17 January 2007; accepted 29 September 2007
Available online 3 December 2007

Abstract

In this paper, the mechanism of limit-cycle excitation is investigated for an aeroelastic system with structural nonlinearities. The analysis is performed on a simplified aeroelastic model retaining only two structural modes (first bending and first torsional modes) and with a simplified description of both unsteady loads due to wing oscillation and external gust excitation. Two cases are considered, without and with gust excitation. In the first case, normal form analysis is employed to give an approximation of the basin of attraction of stable limit cycles in the space of initial conditions. In the second case, a critical gust intensity for a given gust gradient leading again to undamped oscillations is identified.

© 2007 Elsevier Ltd. All rights reserved.

Keywords: Aeroelasticity; Flutter; Limit cycle; Basin of attraction; Normal form

1. Introduction

Aeroelastic systems are typically characterized by a strong coupling between flow and structure that requires a simultaneous description of both of them. Hence, like other fluid–structure interaction problems, aeroelastic systems present a relevant complexity that demands simplified mathematical models and/or reducing techniques. Reduced-order modelling (Dowell et al., 1999) seems to provide a general approach to this effort. It is essentially based on performing high-fidelity simulations (numerical or experimental) of the complex system, thus providing data about the system behaviour from which essential features are extracted. For instance, by projecting the model onto a reduced-space basis, a limited set of generalized coordinates and modes capable of describing the system dynamics is obtained. As outlined above, a rather different approach is the one based on the use of simplifying assumptions to reduce the intrinsic complexity of the problem. This approach has been commonly followed in linear fixed-wing aeroelasticity since the early formulations of the aeroelastic problem and it is based on the following considerations. First, the elastic motion of a cantilevered wing is described with sufficient accuracy by the first bending and torsional modes, thus reducing the structural degrees-of-freedom (dofs). Second, the load acting upon the wing is provided by the spanwise distribution of

*Corresponding author. Tel.: +39 06 50299254; fax: +39 06 5070619.
E-mail addresses: d.dessi@insean.it (D. Dessi), franco.mastroddi@uniroma1.it (F. Mastroddi).

0889-9746/$ - see front matter © 2007 Elsevier Ltd. All rights reserved.
doi:10.1016/j.jfluidstructs.2007.09.003

the lift and pitching moment, assuming that the flow around each wing section is 2-D, incompressible and potential. These concepts were well established at the early stage of aeroelasticity through the concept of typical section, i.e., the reduction of the original problem to the study of the equivalent 2-D section, placed for instance at 70% of the wing span. More recently, a further simplification has been provided by the finite-state formulation of the unsteady aerodynamic loads: a few augmented states (and corresponding differential equations) were demonstrated to be necessary to account satisfactorily for the circulatory lift. In this way, the aeroelastic system can finally be recast in a pure differential form with a very limited set of unknowns. On this basis, in last decades, nonlinear aeroelasticity has broadened the predictive capability of classical aeroelastic models via the inclusion of aerodynamic and structural nonlinearities, providing several interesting applications of both the concepts and numerical/analytical methods developed in the field of nonlinear dynamics.

The most relevant problem that has received renewed attention within fixed-wing aeroelasticity is the prediction of the air-flow condition above which the wing–air system may become unstable. In fact, advanced wing configurations or the deterioration of the airplane control surfaces have required a generalization of the well-established concept of critical speed. Generally speaking, if the instability involves oscillations, the phenomenon is called flutter, otherwise it is called divergence. Accordingly to the linear stability analysis, the oscillations beyond the so-called (linear) flutter speed U_L are not damped and their amplitude grows exponentially, from a mathematical point of view, leading to the collapse of the wing structure. In the case of nonlinear aeroelastic systems, more attention must be paid to the effects that some kinds of nonlinearities may induce on flutter. In Dowell et al. (1997) an exhaustive review of the scenario of nonlinear aeroelastic phenomena was presented. Within this framework, nonlinear torsional stiffness and control-surface freeplay were extensively analysed in the technical literature of the last decade [e.g., see Lee and Tron (1989); Alighanbari and Price (1996); Lee et al. (1998)]. In these papers the nonlinear aeroelastic vibration of a 2-dof pitching and plunging airfoil or 3-dof pitching, plunging airfoil with a control-surface independent rotation was numerically studied and sometimes compared with experimental results.

Focusing on nonlinear aeroelastic systems exhibiting limit-cycle oscillations (LCO), there is well known experimental evidence shown, e.g., in Lacabanne (1997), Matsushita et al. (1998) and Chen et al. (1998), as well as numerical evidence, as shown e.g., in Woolston et al. (1957), Conner et al. (1997) and Dessi and Mastroddi (2004), that a combination of (i) small-amplitude unstable limit cycles (LC) and (ii) large-amplitude stable LC may occur below the linear flutter speed. This implies the possibility, under suitable initial conditions, of *finite* amplitude LCO even below the linear flutter speed. This phenomenon [see Dessi and Mastroddi (2004)] displays a sub-critical Hopf bifurcation exhibiting a so-called turning point at a velocity lower than the (linear) flutter speed, determining a 'knee' in the bifurcation diagram where the unstable LC (sub-critical Hopf bifurcation) reverses into a stable one.

More recently, aeroelastic modelling has considered the combination of nonlinear and stochastic responses via the inclusion of the effects due to flow random perturbations, as done in Poirel and Price (2001). In general, two distinct effects may be identified for an airfoil undergoing a randomly perturbed inflow. In the first case, the perturbation velocity components are orthogonal to the undisturbed flow (vertical gust). In this condition the related aerodynamic forces are independent from the state-space variables (e.g., pitch angle, plunge, modal co-ordinates, etc.) because this perturbation is not coupled with the system behaviour and, therefore, its influence is of one-way type. Therefore, the mathematical model describes these forces directly as an external (stochastic) input. In the second case, the perturbation involves only the flow-wise component of the velocity, thus generating aerodynamic forces that are dependent on the state-space variables. The induced aerodynamic forces cannot be considered as an external (stochastic) input but only as a perturbation of the system parameters. The parametrically excited system does not necessarily need a huge amount of calculations to provide a significant statistics about the solution, since Monte Carlo approaches can be avoided by using, for instance, a stochastic perturbation technique (Carcaterra et al., 2005).

Indeed, the inclusion of vertical gust effects in the aeroelastic modelling provides the physical mechanism by which the wing is actually perturbed in the rest condition. This phenomenon has recently been investigated experimentally providing new insight about how the forced wing response combines with the potential onset of LCO in certain flow speed regimes (Tang et al., 2000; Tang and Dowell, 2002). In particular, in the knee-bifurcation scenario, a vertical gust of adequate intensity might induce LCOs of relevant amplitude even below the linear flutter speed. A basin of attraction of the LC solution in terms of the gust parameters is revealed to actually be more interesting from a physical point of view than that obtained by varying the system initial conditions. In this paper, the oscillations of an aeroelastic typical section (described in terms of plunge and pitch dofs) are analysed with the use of both numerical simulations and a perturbation technique (the normal form method). Particular care is here devoted to investigating the physical mechanism that causes the onset of flow-induced vibrations. Traditionally, the nonlinear analysis concerns the determination of the steady-state solutions (fixed points and both stable and unstable LC) and, eventually, the consequent study of local dynamics, but less attention is dedicated to the identification of the basins of attraction. When the aeroelastic system is described by an autonomous equation (no forcing term), the use of nonlinear techniques like

perturbation methods can help to simplify the governing equations and, in this way, to reduce also the numerical task connected to 'draw' the boundaries of the basins of attraction in the space of initial conditions. On the other hand, when a forcing term like the gust excitation is accounted for, the gust parameters become the key factors that govern the asymptotic evolution and the stability of the solution. Thus, in the present paper, using the discrete gust model (i.e., deterministic and finite-energy input model), the critical gust features determining damped or undamped wing oscillations are identified for several combinations of the gust parameters, i.e., intensity and gradient.

2. Aeroelastic system equations

In this section the governing equations of a 2-dof typical section described in terms of pitching and plunging motion are introduced. The formulation of this problem is obtained as follows. Consider a 2-dof airfoil, elastically constrained by a linear translational spring and a nonlinear torsional spring, oscillating in pitch and plunge. Using standard notations, the plunging deflection is denoted by h, positive in the downward direction, and α is the pitch angle about the elastic axis, positive with nose up. The elastic axis is located at a distance $a_h b$ from the mid-chord, where b is half the chord, while the mass centre is located at a distance $x_\alpha b$ from the elastic axis. Both distances are positive when measured towards the trailing edge of the airfoil. The linear aeroelastic equations of motion are given, for instance, in Fung (1969). In Alighanbari and Price (1996) an extension of these equations to the case in which the torsional spring is nonlinear is available, whereas in Poirel and Price (2001) the authors took into account the combination of unsteady loads due to both airfoil oscillations and incoming gust. Thus, the final governing dimensionless equations are

$$\ddot{\xi} + x_\alpha \ddot{\alpha} + (\bar{\omega}U)^2 \xi = -p_\phi(\tau) - p_\psi(\tau), \quad \frac{x_\alpha}{r_\alpha^2}\ddot{\xi} + \ddot{\alpha} + \frac{1}{U^2} M(\alpha) = r_\phi(\tau) + r_\psi(\tau), \tag{1}$$

where the overdot denotes differentiation with respect to the nondimensional time τ, defined as $\tau = Vt/b$, with V the dimensional speed and b the semi-chord, $\xi = h/b$ is the nondimensional plunge displacement of the elastic axis, $r_\alpha = (J_\alpha/mb^2)^{1/2}$ is the radius of gyration about the elastic axis; note that $M(\alpha)$ is the overall expression of the torsional spring moment, including the linear part. In Eqs. (1), $\bar{\omega}$ is given by $\bar{\omega} = \omega_\xi/\omega_\alpha$ where ω_ξ and ω_α are the uncoupled plunging and pitching modes natural frequencies, and U is the nondimensional air speed defined as $U = V/b\omega_\alpha$. Moreover, $p_\phi(\tau)$ and $r_\phi(\tau)$ are the lift and pitching moment due to airfoil motion, respectively, and $p_\psi(\tau)$ and $r_\psi(\tau)$ are the lift and pitching moment due the gust profile, respectively. For incompressible 2-D flow, Fung (1969) gives the following expressions for $p_\phi(\tau)$ and $r_\phi(\tau)$ in the case of zero initial conditions:

$$\begin{aligned} p_\phi(\tau) &= \frac{1}{\bar{\mu}}(\ddot{\xi} - a_h\ddot{\alpha} + \dot{\alpha}) + \frac{2}{\bar{\mu}}\int_0^\tau \phi(\tau-\sigma)\dot{w}_{3/4}(\sigma)\,\mathrm{d}\sigma, \\ r_\phi(\tau) &= \frac{1}{\bar{\mu}r_\alpha^2}\left[a_h(\ddot{\xi} - a_h\ddot{\alpha}) - \bar{a}_h\dot{\alpha} - \frac{1}{8}\ddot{\alpha}\right] + \frac{2}{\bar{\mu}r_\alpha^2}\left(\frac{1}{2} + a_h\right)\int_0^\tau \phi(\tau-\sigma)\dot{w}_{3/4}\,\mathrm{d}\sigma, \end{aligned} \tag{2}$$

where $\bar{\mu} = \pi\rho b^2/m$ is the mass ratio, $w_{3/4}(\tau) = \dot{\xi}(\tau) + \bar{a}_h\dot{\alpha}(\tau) + \alpha(\tau)$ and $\bar{a}_h = 1/2(1 - a_h)$ is the downwash, with $\phi(\tau)$ the Wagner function. The expressions for $p_\psi(\tau)$ and $r_\psi(\tau)$ are

$$\begin{aligned} p_\psi(\tau) &= \frac{2}{\bar{\mu}}\left(w_G(0)\psi(\tau) + \int_0^\tau \psi(\tau-\sigma)\dot{w}_G(\sigma)\,\mathrm{d}\sigma\right), \\ r_\psi(\tau) &= \frac{2}{\bar{\mu}r_\alpha^2}\left(\frac{1}{2} + a_h\right)\left(w_G(0)\psi(\tau) + \int_0^\tau \psi(\tau-\sigma)\dot{w}_G\,\mathrm{d}\sigma\right), \end{aligned} \tag{3}$$

where $w_G(\tau)$ is the vertical gust velocity at 1/4-chord and $\psi(\tau)$ is the Kussner function (Fung, 1969).

3. Finite-state modelling for nonlinear gust problem

Because of the existence of the integral term in the expression of aerodynamic forces (Eqs. (2) or (3)), classical methods to investigate stability properties of dynamical systems do not work: for instance, the system stability near equilibrium points cannot be analysed readily since most of the available methods for nonlinear dynamical systems are developed for ordinary differential equations in the form $\dot{\mathbf{x}} = \mathbf{F}(\mathbf{x}, t)$. The mathematical procedure to avoid the convolution integral term has been applied to several systems in literature. It is essentially based on defining additional variables and equations describing their evolution. In the field of aeroelasticity, this approach to the description of the

circulatory part of the aerodynamic loads is known as aerodynamic finite-state modelling. The definition of the augmented or lag state for the circulatory part of the gust lift follows the procedure adopted in Dessi et al. (2002) for the unsteady lift due to wing motion; thus introducing

$$u(\tau) = \int_0^\tau \phi(\tau - \sigma)\dot{w}_{3/4}(\sigma)\,\mathrm{d}\sigma, \tag{4}$$

the augmented state relative to the unsteady lift due to the gust excitation is similarily defined as

$$v(\tau) = w_G(0)\psi(\tau) + \int_0^\tau \psi(\tau - \sigma)\dot{w}_G(\sigma)\,\mathrm{d}\sigma. \tag{5}$$

The aim of successive algebraic manipulations in the Laplace domain (all the equations are Laplace-transformed) is to re-write these relationships as differential equations in the unknown function $u(\tau)$ and $v(\tau)$. In the following, Laplace-transformed terms will be denoted by a tilde, while the Laplace variable is denoted by s.

Skipping the derivation of the equation for the augmented state $u(\tau)$ [see Dessi and Mastroddi, 2004 for details], let us consider Eq. (5), that is integrated by parts, thus providing

$$v(\tau) = \int_0^\tau w_G(\sigma)\dot{\psi}(\tau - \sigma)\,\mathrm{d}\sigma. \tag{6}$$

Applying Laplace transformation to the above equation yields

$$\tilde{v}(s) = s\tilde{\psi}(s)\tilde{w}_G(s), \tag{7}$$

whereas the finite state, namely, the two-state representation of the Kussner function in the Laplace domain is

$$\tilde{\psi}(s) = \frac{1}{s} - \frac{\check{a}}{s + \check{b}} - \frac{\check{c}}{s + \check{d}} = \frac{\tilde{N}(s)}{\tilde{D}(s)} \tag{8}$$

with $\check{a} = 0.5792$, $\check{b} = 0.1393$, $\check{c} = 0.4208$ and $\check{d} = 1.802$ (Blishplinghoff et al., 1996). Substituting Eq. (8) into Eq. (7), one obtains

$$\frac{\tilde{D}(s)}{s}\tilde{v}(s) = \tilde{D}_1(s)\tilde{v}(s) = \tilde{N}(s)\tilde{w}_G(s), \tag{9}$$

where $\tilde{D}_1(s)$ is equal to $s\tilde{D}(s)$. As expected, the equation for the lag state $v(\tau)$ is not coupled with other equations and it provides only at each time instant the excitation due to the circulatory lift associated with the gust (on the other hand, the final equation for $u(\tau)$ is much more complicated because the downwash $w_{3/4}$ couples this equation with the pitch and plunge equations).

A simple but enlightening hypothesis for the atmospheric (deterministic) gust is a vertical velocity distribution of the form

$$w_G(\tau) = \frac{w_0}{2}\left(1 - \cos\frac{\pi\tau}{\tau_G}\right) \quad \text{for } 0 \leqslant \tau \leqslant 2\tau_G, \tag{10}$$

$$w_G(\tau) = 0 \quad \text{for } \tau > 2\tau_G, \tag{11}$$

where w_0 represents the peak gust velocity and τ_G represents the gust gradient expressed in half-chord unit lengths. The Laplace transformation of $w_G(\tau)$ is (here the hypothesis of causality for the function $w_G(\tau)$ has been made, i.e., $w_G(\tau) = 0$ for $\tau < 0$)

$$\tilde{w}_G(s) = w_0\left(\frac{\pi}{\tau_G}\right)^2 \frac{1}{s(s^2 + (\pi/\tau_G)^2)}(1 - \mathrm{e}^{-2\tau_G s}). \tag{12}$$

Setting again

$$\check{e}_{10} = \check{b} + \check{d}, \quad \check{e}_{11} = \check{b}\check{d}, \quad \check{e}_{12} = \check{b} + \check{d} - \check{b}\check{c} - \check{a}\check{d}, \quad \check{e}_{13} = 1 - \check{a} - \check{c},$$

one obtains

$$(s^2 + \check{e}_{10}s + \check{e}_{11})\tilde{v}(s) = (\check{e}_{13}s^2 + \check{e}_{12}s + \check{e}_{11})\left[w_0\left(\frac{\pi}{\tau_G}\right)^2 \frac{1}{s(s^2 + (\pi/\tau_G)^2)}(1 - \mathrm{e}^{-2\tau_G s})\right]. \tag{13}$$

The inverse transformation of the right-hand side (r.h.s) of Eq. (13) gives the following form:

$$\ddot{v} + e_{10}\dot{v} + e_{11}v = g(t), \tag{14}$$

where the forcing term in the r.h.s. is

$$\begin{cases} g(t) = e_{11}\dfrac{w_0}{2}\left(1 - \cos\dfrac{\pi\tau}{\tau_G}\right) + e_{12}\dfrac{w_0\pi}{2\tau_G}\sin\dfrac{\pi\tau}{\tau_G} + e_{13}\dfrac{w_0\pi^2}{2\tau_G^2}\cos\frac{\pi\tau}{\tau_G}, & \text{for } \tau \leqslant 2\tau_G, \\ g(t) = 0, & \text{for } \tau > 2\tau_G. \end{cases} \tag{15}$$

Finally, the problem may be recast as a system of eight first-order differential equations, as

$$\dot{\mathbf{x}} = \mathbf{A}(U)\mathbf{x} + \mathbf{f}(\mathbf{x}; U) + \mathbf{g}(t; U), \tag{16}$$

where $\mathbf{x} = \{\dot{\xi}, \dot{\alpha}, \dot{u}, \dot{v}, \xi, \alpha, u, v\}^{\mathrm{T}}$ is the state vector, $\mathbf{A}(U)$ is the linear part of the equations of motion, $\mathbf{f}(\mathbf{x}; U)$ is the vector of nonlinear terms (structural nonlinearities) and $\mathbf{g}(t; U)$ is the external excitation due to the vertical gust profile. It is usual to recast the system also in complex pseudo-diagonal form, introducing the state-space vector $\mathbf{z} = \mathbf{R}\mathbf{x}$, so that $\mathbf{A}(U_L)\mathbf{R} = \mathbf{R}\mathbf{\Lambda}$. In this case, the equation takes the form

$$\dot{\mathbf{z}} = \mathbf{\Lambda}(U)\mathbf{z} + \hat{\mathbf{f}}(\mathbf{z}; U) + \hat{\mathbf{g}}(t; U), \tag{17}$$

where $\mathbf{\Lambda}$, $\hat{\mathbf{f}}$ and $\hat{\mathbf{g}}$ are the transformed terms in the right eigenvector basis.

4. Results

The values of the system coefficients considered in this paper are

$$\mu = 100, \quad x_\alpha = 0.25, \quad \bar{\omega} = 1.2, \quad r_\alpha = 0.5, \quad \text{and} \quad a_h = -0.5.$$

First, consider how the aeroelastic system loses (linear) stability as the inflow velocity (or the flight speed) U is increased. The flutter speed and frequency are obtained by a standard eigenanalysis. The critical speed obtained is $U_L = 4.9371$ (flutter speed), whereas $\omega_L = 0.255$ is the critical frequency associated with the pair of complex eigenvalues transversely crossing the imaginary axis at U_L. The system nonlinearity, that accounts for the presence of a nonlinear torsional stiffness, is expressed as

$$M(\alpha) = \alpha + \beta_3\alpha^3, \tag{18}$$

where $\beta_3 = -50$.

4.1. Nonlinear response to given initial conditions

First, the system nonlinear behaviour is analysed assuming $w_G = 0$, i.e., in the absence of a vertical gust. In this case, the system does not contain any forcing function, i.e., $\mathbf{g}(t) = 0$; and, supposing that the effects of any previous gust were damped out, one has $v(0) = \dot{v}(0) = 0$. Similarly, it is supposed that the system starts to evolve from a 'frozen' configuration (no unsteady lift for $\tau \leqslant 0$), and it is set also $u(0) = \dot{u}(0) = 0$. Initial conditions are then applied only to the pitch and plunge variables. Since $\beta_R = \mathbf{l}^{\mathrm{T}}\mathbf{A}(U_L)\mathbf{r} < 0$ and $\gamma_R = \mathbf{l}^{\mathrm{T}}\hat{\mathbf{f}}(\mathbf{r}; U) > 0$ ($\mathbf{r}$ and $\mathbf{l}$ are the critical right and left eigenvectors, respectively), one has $A_{LC}^2 = -\beta_R/\gamma_R > 0$ and the system is subjected to a subcritical Hopf bifurcation (Chow and Hale, 1982).

In previous works [see, e.g., Dessi et al. (2002)] the parameter a_h was revealed as a key parameter for the description of the pre-critical bifurcation scenario. Indeed, varying the value of such a parameter from -0.4 to -0.5 the bifurcation diagram exhibited the onset of an unstable LCO. More specifically, for a value of the parameter a_h less than about -0.48, a pre-critical Hopf bifurcation occurred; in other words, in this case, although the speed velocity is less than the linear stability value U_L, the system exhibits a stable (trivial) equilibrium solution for all the initial conditions in the state space up to a threshold (namely, the unstable LC). For initial conditions that are beyond such a threshold a stable LCO is reached by the state-space vector. This description is valid for decreasing the value of U up to a lower limit, U_T, under which the LC behaviour (both, stable and unstable regions) disappears. The margin given by U_T denotes a turning point, a point where the stable and the unstable linearly pre-critical LC branches merge. From an aeroelastic point of view, this represents the lowest value of the flight speed U for which an instability may occur (given suitable initial conditions or, as will be examined later, a proper gust excitation). It is worth to recall that U_T does not depend on the value of the nonlinearity, i.e., on β_3. In general, the information provided from the curve of the LCOs allows to

analyse the system asymptotic behaviour but does not provide any indication about the set of initial conditions that determines a damped or undamped behaviour. In order to consider such a rich bifurcation scenario in the next application, a value of $a_h = -0.5$ has been taken into account.

For this purpose, using suitable techniques the state space can be divided into several regions that constitute the basins of attraction of the asymptotic solutions. A trivial approach is to generate a uniform grid in the state space, thus using the value of the state vector at the nodes, say $\mathbf{x}_0^{(i)}$, as the vector of initial conditions for the corresponding simulation. Another possibility is to use a Monte-Carlo approach to generate a population of initial value problems, each one characterized by a randomly chosen $\mathbf{x}_0^{(i)}$. A more sophisticated approach, based on Poinaré maps and embedded state vector, was also proposed by Trickey et al. (2002). Indeed, the previous approaches involve a heavy numerical burden if they are applied on the original full-system equations.

On the other hand, the system equations can be further analysed so as to try to reduce their order and thus to obtain information about the basins of attraction, following the procedure described in Dessi et al. (2002). In fact, the Hopf bifurcation theorem prescribes the presence of a 2-D centre manifold in the neighbourhood of the flutter speed U_L. Thus, using near-identity transformations of the form (Wiggins, 1990)

$$\mathbf{z} = \mathbf{y} + \mathbf{W}(\mathbf{y}), \tag{19}$$

with $\mathbf{W}(\mathbf{y})$ the nonlinear part of the transformation, it follows that the system dynamics is well approximated by the normal form equations

$$\begin{aligned}
\dot{y}_1 &= \mathrm{i}\,\omega_L y_1 + (U_L - U)\sum_{p=1}^{2}\alpha_{1p}y_p + \sum_{pqr=1}^{2}\gamma_{1pqr}y_p y_q y_r,\\
\dot{y}_2 &= -\mathrm{i}\,\omega_L y_2 + (U_L - U)\sum_{p=1}^{2}\bar{\alpha}_{1p}y_p + \sum_{pqr=1}^{2}\bar{\gamma}_{2pqr}y_p y_q y_r.
\end{aligned} \tag{20}$$

The dynamics described by Eq. (20) belongs to the phase plane of the real unknowns $\mathscr{R}e[y_1] = (y_1 + y_2)/2$—the real part of y_1—and $\mathscr{I}m[y_1] = (y_1 - y_2)/2\mathrm{i}$—the imaginary part of y_1. Therefore, the unstable LC curve $\mathbf{x}_u^{(\mathrm{LC})}(t)$ for each value of U divides the plane into two regions (inside and outside the unstable orbit) that constitute the basins of attraction of the fixed point solution $\mathbf{y} = \mathbf{0}$ and of the stable LC curve $\mathbf{y}_s^{(\mathrm{LC})}(t)$. By projecting the unstable LC solution onto the physical state space, one obtains a curve $\mathbf{x}_u^{(\mathrm{LC})}(t) = \mathbf{l}^{\mathrm{T}}\mathbf{y}_u^{(\mathrm{LC})}(t)$ that is the boundary between the two basin of attractions.

Equation (20) is obtained with a third-order normal form analysis. As long as the system dynamics evolves far form the critical point (both in magnitude of the vector $\mathbf{y}$ and parameter $U_L - U$) the third-order approximation fails even qualitatively. Indeed, the presence of the turning point implies that resonant terms of higher order—at least fifth-order terms—have to be retained with the normal form analysis. In Dessi et al. (2002) it is shown that the inclusion of fifth-order terms surely improves the qualitative behaviour of the solution (change of the LC stability at the turning point), but there is still a lack of accuracy of the normal form solution in terms of amplitude of the LC. This unsatisfactory approximation is not dependent uniquely on the order of the normal form analysis, but it is due also to the fact that the coordinates y_1 and y_2 are no longer sufficient to describe the system dynamics, especially as long as the turning point is approached.

This issue was investigated in Dessi et al. (2002) by introducing a quantity, evaluated at $U = U_L$, designated as the $\hat{\lambda}$-point and defined as

$$\hat{\lambda} = \hat{\lambda}(i, j_1, \ldots, j_m) = \lambda_i - \mathbf{a}^{\mathrm{T}}\boldsymbol{\lambda}, \tag{21}$$

where $\boldsymbol{\lambda}^{\mathrm{T}} = \{\lambda_1, \lambda_2, \ldots, \lambda_N\}$ and $\mathbf{a}^{\mathrm{T}} = \{a_1, a_2, \ldots, a_N\}$, with a_i are positive integer number assuming that $\mathrm{Tr}[\mathbf{a}] = q$ is the order of terms considered for the perturbation analysis. In an analogous way to linear analysis, where an eigenvalue (or frequency) is associated to each linear term (or mode), using the above relationship it is possible to associate to each nonlinear term a combination of the (linear) system eigenvalues.

Then, the assumption that only the $\hat{\lambda}$-points satisfying the condition $|\lambda_i - \mathbf{a}^{\mathrm{T}}\boldsymbol{\lambda}| < \rho$ are to be considered as 'near-resonant' simply implies that only the corresponding nonlinear terms have to be retained in the equations (this condition appears as an extension of the classical resonant condition, $\lambda_i - \mathbf{a}^{\mathrm{T}}\boldsymbol{\lambda} = 0$). The value ρ of the radius was determined with a trial and error procedure. Specifically, if we increased the number of $\hat{\lambda}$-points, no difference was observed; on the other hand, if any of the $\hat{\lambda}$-points in the minimal set was removed, substantial deterioration was

obtained—indeed, for some choices, instabilities were observed. Thus the equations used are

$$\dot{y}_1 = \sum_{p\in I_{1,1}} a_{1p}y_p + \sum_{pqr\in I_{1,3}} c_{1pqr}y_p y_q y_r + \sum_{pqrst\in I_{1,5}} e_{1pqrst}y_p y_q y_r y_s y_t,$$
$$\dot{y}_3 = \sum_{p\in I_{3,1}} a_{3p}y_p + \sum_{pqr\in I_{3,3}} c_{3pqr}y_p y_q y_r + \sum_{pqrst\in I_{3,5}} e_{3pqrst}y_p y_q y_r y_s y_t, \tag{22}$$

where $y_2 = \dot{y}_1$, and $y_4 = \dot{y}_3$ (the index combinations $I_{i,q}$ are reported in Dessi et al., 2002, providing a clear improvement of both the time-history solution and LCO amplitudes for each considered value of the flow speed U. Indeed, it is worth to consider that only a few index combinations provide nonzero coefficients, thus decreasing significantly the computational cost.

4.2. Nonlinear response to gust input

Though interesting from a mathematical point of view, the determination of the basins of attraction from given initial conditions in the state space does not provide practical information about the possibility that LCOs might be reached below the flutter speed. Usually, the physical mechanism that makes the wing to vibrate is due to airplane manoeuvering and/or to gust occurrence. In the second case, it is reasonable to expect that the intensity and duration of the gust may affect the solution and its asymptotic behaviour. Therefore, the analysis of the flutter occurrence (in a general sense) should explore the dynamics of the wing structure for all the combinations of the parameters describing the gust. If the gust model $g(t)$ is provided, the equations of motions become of the form given by Eq. (16). The solution of Eq. (16) is numerically obtained with a Runge–Kutta method by using zero initial conditions and a discrete '1-Cosine' gust model. Within this assumption, for a given flow velocity U, the two parameters on which the solution depends are therefore the gust intensity w_0 and the gust gradient τ_G. Thus, the final scope of this analysis is to determine the basin of attraction of the solution in the plane (w_0, τ_G) for each flow velocity U.

Indeed, this task would require again an intensive numerical simulation even if only the velocities corresponding to the subcritical range $U_T \leqslant U \leqslant U_L$ are considered. Therefore, the following procedure is adopted. First, the gust gradient represented by τ_G is set to a prescribed value, e.g., $\bar{\tau}_G$, in the range of the admissible values. Then, the flow velocity range (U_T, U_L) is spanned with a certain step ΔU. For each velocity U, the system solution after a period $\tau_N \gg \tau_G$ will be damped or undamped. Ideally, it is possible to identify the critical gust intensity $w_0(U, \tau_G)$ that brings the solution over the unstable LC (numerically, the solution will be very close to it for $\tau \leqslant \tau_N$). Thus, defining at the time instant τ_N the logarithmic decay ratio η_N as

$$\eta_N(U, w_0, \tau_G) = \ln \frac{x_N^{(i)} - x_{N-1}^{(i)}}{\tau_N - \tau_{N-1}}, \tag{23}$$

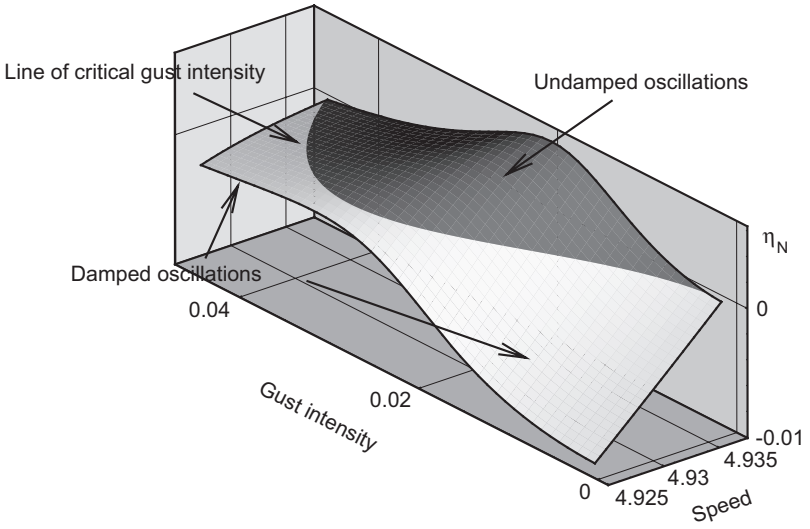

Fig. 1. Logarithmic damping η_N after 2000 time steps.

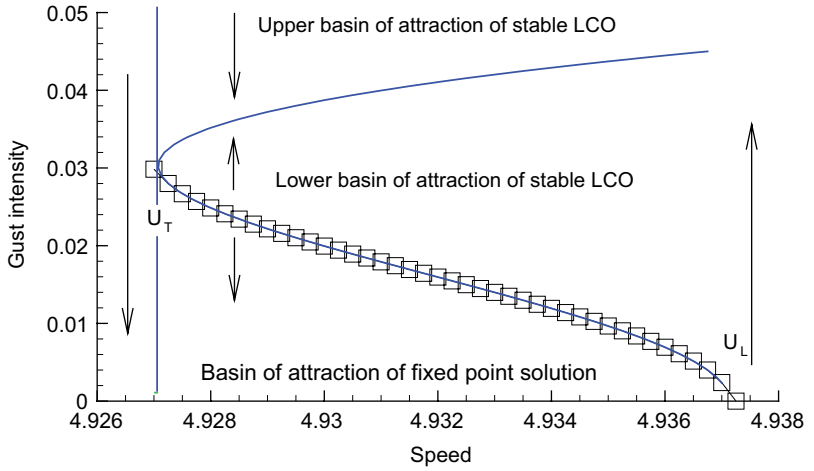

Fig. 2. Basins of attraction of the stationary solutions and critical gust intensity at a gust gradient $\tau_G = 10$.

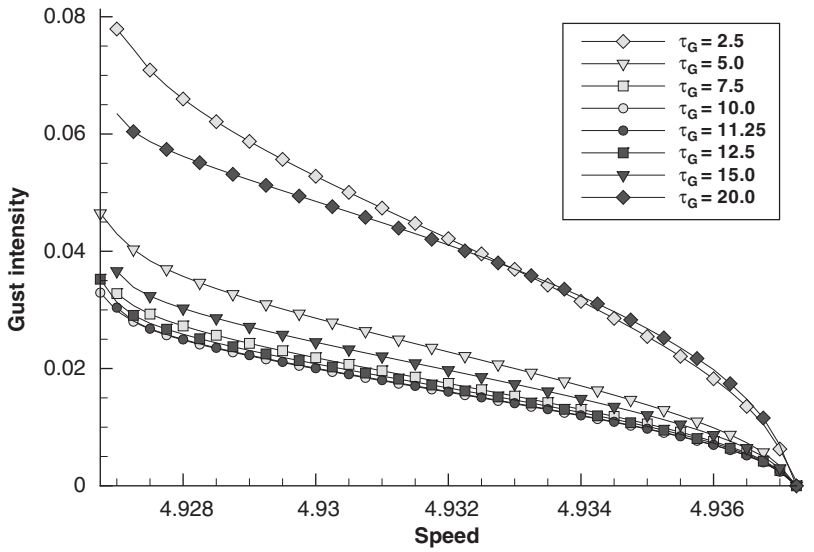

Fig. 3. Several curve at various gust gradients for the critical gust intensity.

where $x_N^{(i)}$ is the peak (maximum or minimum) corresponding to the $x^{(i)}$ state variable and $(\tau_N - \tau_{N-1})$ is the time interval between consecutive maxima. The resulting 2-D surface $\eta_N(U, w_0; \bar{\tau}_G)$ is then plotted as done in Fig. 1. In dark shade the region has been highlighted corresponding to combination of speed and gust intensity that determines undamped solution (really approaching the stable LC), whereas in lighter shade is indicated the region related to a damped solution (no matter if the system goes to LC or fixed point solutions). The curve in the plane (U, w_0) representing the solution of the equation $\eta_N(U, w_0; \bar{\tau}_G) = 0$ can simply be drawn by considering the level 0 of the contour plot shown in Fig. 1, thus obtaining the solid curve of Fig. 2. In the present calculations, more precisely, the points of the curve described above are obtained by using the secant method to solve the previous equation in the unknown w_0 for each selected flow velocity U, i.e.,

$$w_0^{(j+1)} = w_0^{(j)} - \eta_N(w_0^{(j)}) \frac{w_0^{(j)} - w_0^{(j-1)}}{\eta_N(w_0^{(j)}) - \eta_N(w_0^{(j-1)})}.$$

In Fig. 2 the curve of the critical gust intensity, obtained with the numerical scheme introduced above, is plotted with respect of U. If a gust intensity is chosen below this curve, the solution tends to be damped out; otherwise, the solution

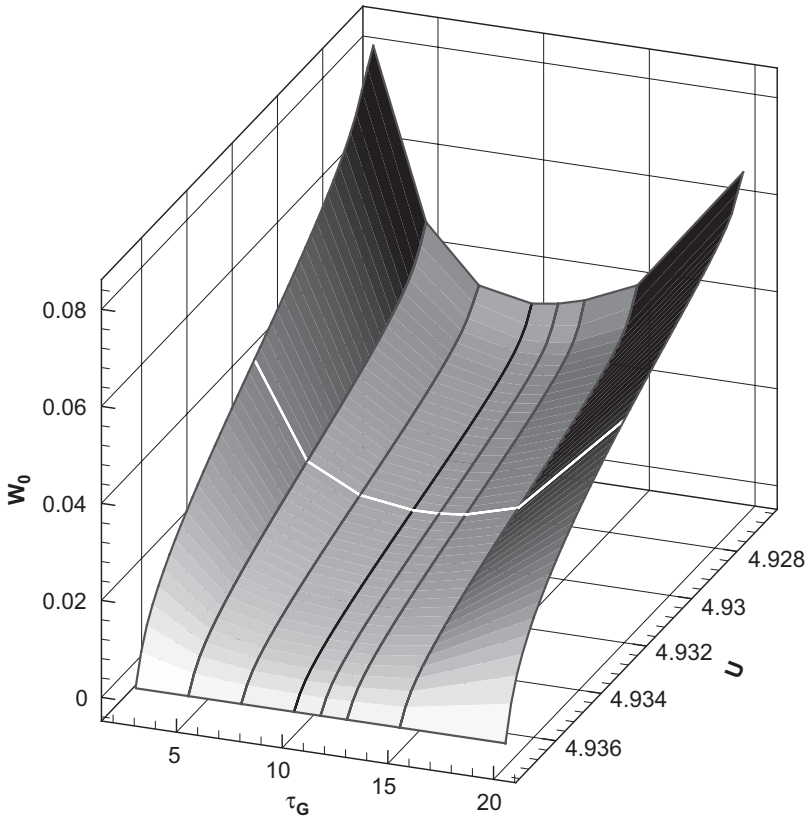

Fig. 4. Three-dimensional representation of the dependence of the critical gust intensity upon speed and gust gradients.

reaches the stable LC solution. Next, consider how this curve depends on the gust gradient. This is shown for several gust gradients in Figs. 3 and 4. It is interesting to note that for $\tau_G \to \infty$ the critical gust intensity grows for every flight speed considered, indicating a safe condition. In fact, in this case the gust effect induces a series of quasi-steady states that differ from each other for the equilibrium solution, that is no more equal to zero (a constant vertical gust would determine a constant angle of attack, then the equation would no longer be homogeneous). When the τ_G is decreased, its duration becomes comparable to the system time constants, and the critical gust intensity reaches globally a local minimum (worst gust condition, curves with circles in Fig 3). The presence of a minimum with respect to τ_G is also apparent looking at Fig. 4, where for $U = 4.932$ the section $w_0(\tau_G)$ is highlighted in white. On the other hand, for $\tau_G \to 0$ the critical gust intensity for each flow velocity tends to a finite value because the effect of a very short gust is just to move the initial conditions to a prescribed value.

5. Concluding remarks

In the present paper the basins of attraction of a nonlinear aeroelastic system subjected to a vertical gust load has been investigated. A preliminary stability analysis using a normal form perturbation approach has been carried out and it has shown the occurrence of a pre-critical Hopf bifurcation. Next, the nonlinear gust response analysis has been performed and the basin of attraction of the solution as function of gust profile parameters has been presented. The results presented in this paper encourage further investigation on the dependence of the LC solutions on the gust profile. The excitation due to discrete gust models surely is equivalent to considering the response of the system to certain initial conditions belonging to a particular basin of attraction. If a continuous or stochastic gust is considered, the system dynamics may be deeply different from the one examined in this paper. Moreover, the analysis of transient states need also to be carefully analysed because they might be significantly affected by resonant phenomena when the gust duration is comparable with the system time constants.

Acknowledgement

This work has been supported in the frame of the INSEAN research program Programma Ricerche 2006-08.

References

Alighanbari, H., Price, S.J., 1996. The post-Hopf-bifurcation response of an airfoil in incompressible two-dimensional flow. Nonlinear Dynamics 10, 381–400.

Blishplinghoff, R.L., Ashley, H., Halfman, R.L., 1996. Aeroelasticity. Dover Publications, New York.

Carcaterra, A., Dessi, D., Mastroddi, F., 2005. Hydrofoil vibration induced by a random flow: a stochastic perturbation approach. Journal of Sound and Vibration 283 (1–2), 401–432.

Chen, P.C., Sarhaddi, D., Liu, D.D., 1998. Limit-cycle-oscillations studies of a fighter with external stores. AIAA-98-1727, pp. 258–266.

Chow, S., Hale, J.K., 1982. Methods of Bifurcation Theory. Springer, New York.

Conner, M.D., Tang, D.M., Dowell, E.H., Virgin, L.N., 1997. Nonlinear behavior of a typical airfoil section with control surface with freeplay: a numerical and experimental study. Journal of Fluids and Structures 11, 89–109.

Dessi, D., Mastroddi, F., 2004. Limit-cycle stability reversal via singular perturbation and wing-flap flutter. Journal of Fluids and Structures 19, 765–783.

Dessi, D., Morino, M., Mastroddi, F., 2002. Limit-cycle stability reversal near a hopf bifurcation with aeroelastic applications. Journal of Sound and Vibration 256 (2), 347–365.

Dowell, E.H., Virgin, L.N., Tang, D.M., Conner, M.D., 1997. Nonlinear dynamics of aeroelastic systems. In: Proceedings of International Forum on Aeroelasticity and Structural Dynamics, Rome, Italy, pp. 79–91.

Dowell, E.H., Hall, K.C., Thomas, J.P., Florea, R., Epureanu, B.I., Heeg, J., 1999. Reduced order models in unsteady aerodynamics. AIAA-99-1261.

Fung, Y.C., 1969. An Introduction to the Theory of Aeroelasticity. Dover Publications, New York.

Lacabanne, M., 1997. An experimental analysis of the aeroelastic behaviour with a freeplay in a control surface. In: Proceedings of the CEAS International Forum of Aeroelasticity and Structural Dynamics, vol. 3, Rome, pp. 239–246.

Lee, B.H.K., Tron, A., 1989. Effects of structural nonlinearities on flutter characteristics of the CF-18 aircraft. Journal of Aircraft 26 (8), 781–786.

Lee, B.H.K., Jiang, L., Wong, Y.S., 1998. Flutter of an airfoil with a cubic nonlinear restoring force. AIAA-98-1725, pp. 237–257.

Matsushita, H., Saitoh, K., Granasy, P., 1998. Wind tunnel investigation of transonic limit cycle flutter. AIAA-98-1728, pp. 267–273.

Poirel, D.C., Price, S.J., 2001. Structurally nonlinear fluttering airfoil in turbulent flow. AIAA Journal 39 (10), 1960–1968.

Tang, D., Dowell, E.H., 2002. Experimental and theoretical study of gust response for high-aspect-ratio wing. AIAA Journal 40 (3), 419–429.

Tang, D., Henry, J.K., Dowell, E.H., 2000. Nonlinear aeroelastic response of delta wing to periodic gust. Journal of Aircraft 37 (1), 155–164.

Trickey, S.T., Virgin, L.N., Dowell, E.H., 2002. The stability of limit-cycle oscillations in a nonlinear aeroelastic system. Proceedings of the Royal Society 454 (2025), 2203–2226.

Wiggins, S., 1990. Introduction to Applied Nonlinear Dynamical Systems and Chaos. Texts in Applied Mathematics. Springer, New York.

Woolston, D.S., Runyan, H.L., Andrews, R.E., 1957. An investigation of certain types of structural nonlinearities on wing and control surface flutter. Journal of the Aeronautical Sciences 24, 57–63.